INTERNATIONAL JOURNAL OF FLUID POWER, 2018
VOL. 19, NO. 1, 27–41
https://doi.org/10.1080/14399776.2017.1374140

Taylor & Francis
Taylor & Francis Group

Model-based simulation of hydraulic hoses in an intelligent environment

Gunnar Grossschmidt[a] and Mait Harf[b]

[a]Department of Mechanical and Industrial Engineering, Tallinn University of Technology, Tallinn, Estonia; [b]Department of Software Science, Tallinn University of Technology, Tallinn, Estonia

ABSTRACT

In this paper, comprehensive mathematical models of hydraulic hoses for fluid power systems and a modelling and simulation technology based on using multi-pole models and intelligent simulation environment are proposed. Principles of composing multi-pole mathematical models for hydraulic hoses with lumped parameters having various causalities are discussed. Computing transient and frequency responses of hydraulic hoses in a visual simulation tool CoCoViLa are considered. The CoCoViLa environment is a visual programming tool, which supports declarative programming in a high-level language and automatic program synthesis. The proposed technology enables to find optimal solutions for hydraulic hoses in design and development of various fluid power systems.

ARTICLE HISTORY
Received 30 March 2017
Accepted 24 August 2017

KEYWORDS
Hydraulic hose; multi-pole mathematical model; CoCoViLa simulation environment; visual task description; automatic program synthesis

1. Introduction

A hydraulic hose is an environment for energy transfer and transmitting signals in fluid power systems. The hydraulic hoses compensate the relative movement, replace the complicated bent tubes, reduce the pressure pulsation and prevent the forwarding of vibrations. Dynamic phenomena of hydraulic hoses have an influence on the dynamic behaviour of fluid power systems. Design of a hydraulic hose is shown in Figure 1.

The hydraulic hose typically consists of four elements: soul of hose, braids (1, 2, 4, 6 layers), cover of hose and fittings (nipple and socket). Braid is composed of a number of wires wrapped helically around the hose in a basket weave fashion and fixed to the hose at both ends. The angle between crossing wires is called braiding angle. Researchers have dealt with problems of hydraulic transmission lines for a long time. A number of research papers are concerned with the investigation of fluid transmission lines with distributed parameters. Exact models of a distributed parameter system are considerably troublesome to develop simulation programs for the reason that they involve Bessel and hyperbolic functions. It requires work with modal approximations. In (Muto *et al.* 1996), a method has been introduced for simulating the transient response of viscoelastic transmission lines. Irrational functions for describing transfer matrix elements were approximated with high accuracy by rational polynomials. Various lumped parameter models and their solutions have been used to reduce complexity of dynamic analysis (Korobochkin and Komitowski 1968, Stecki and Davis 1986, Krus *et al.* 1994, Taylor *et al.* 1997, Kajaste 1998, Mäkinen *et al.* 2000, Manning 2005, Soumelidis *et al.* 2005, Kojima *et al.* 2006, Pršić *et al.* 2011, Watton 2014).

Frequency characteristics are widely used to describe dynamic behaviour of hydraulic transmission lines (Grossschmidt 1971, Grossschmidt and Vanaveski 1971, Sänger 1985, Xu *et al.* 2014).

Linear models with distributed parameters are suitable for calculating frequency characteristics of tubes (Grossschmidt 1971, Stecki and Davis 1986). Frequency characteristics of large fluid power systems can be directly calculated only in case of linear models of components. In case of non-linear models of components frequency characteristics can be calculated only using transient responses.

When calculating dynamic transient responses of large fluid power systems it is preferable to use non-linear simple models with lumped parameters for hydraulic transmission lines to save calculation resources.

Approximate models with distributed parameters can be considered consisting of a couple of similar models with lumped parameters. In this way, we take into account several natural frequencies of the transmission line.

Our objective is to propose non-linear models with lumped parameters and with various causalities that can be used as components in modelling and simulation of fluid power systems. The aim of the current research is to make the computer simulation of large and complex fluid power systems easier, more precise and faster.

CONTACT Gunnar Grossschmidt gunnar.grossschmidt@ttu.ee

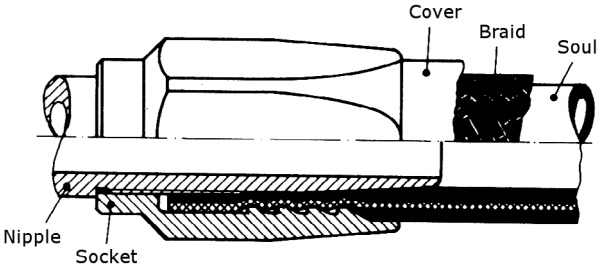

Figure 1. Design of a hydraulic hose.

A hydraulic hose can be considered as a tube with viscoelastic walls. The mathematical models of hoses are quite complex, it makes difficult using them in simulation of fluid power systems (Sänger 1985, Chipperfield and Vance 2002, Kannisto and Virvalo 2002, Johnston 2006, Johnston *et al.* 2010 Ohashi and Hayashi 2014, Speicher *et al.* 2014). Radial and longitudinal deformations of hoses depend on the material of soul and on the construction of braid (material of wire and braiding angle). In practice hoses with minimal longitudinal deformations are manufactured (Sänger 1985). Therefore, in the current paper we concentrate only on radial deformation of hoses.

Multi-pole mathematical models are used for describing hydraulic hoses. Fundamentals of multi-pole model construction principles and methods have been described in (Grossschmidt and Harf 2009). Models of hoses are based on models of hydraulic tubes (Grossschmidt and Harf 2010).

A modelling and simulation technology is proposed for calculating dynamic transient and frequency responses of hydraulic hoses. A visual simulation environment CoCoViLa (Grigorenko *et al.* 2005, Kotkas *et al.* 2011) is used as a tool.

The special features of the used technology are as follows:

- composing multi-pole mathematical models with graphical representation;
- using visual programming and automatic program synthesis for composing and solving simulation tasks;
- using multi-level distributed calculations.

2. Mathematical model of radial deformation of hose wall

Equation of mean radial deformation of hose wall static and steady state model considering hysteresis

$$x = (p\_m \cdot A) / k - b \cdot \text{signv}(v, v\_lim), \quad (1)$$

where arithmetic mean pressure

$$p\_m = (p1 + p2)/2, \quad (2)$$

inner area of hose

$$A = \pi \cdot (d + 2 \cdot x) \cdot l. \quad (3)$$

Radial stiffness of the hose wall is non-linear, depending on hose wall material, construction of braid and pressure. At lower pressures the stiffness is lesser.

The stiffness is characterised by reference deformation *x_ref* at reference pressure *p_ref* and ratios of stiffnesses *k* at *p_m* = *p_ref* and *k* at *p_m* = 0.

The graphical dependence of hose wall stiffness *k* on pressure *p_m* (Murrenhoff 2005, Figure 2.4–5) is estimated to match the best way as logarithmic

$$k = k\_ref/3 \cdot (1 + \log(90 \cdot p\_m/p\_ref + 10)), \quad (4)$$

where reference radial stiffness of the hose wall

$$k\_ref = (p\_ref \cdot A\_ref) / x\_ref, \quad (5)$$

reference hose inner area

$$A\_ref = \pi \cdot (d + 2 \cdot x\_ref) \cdot l. \quad (6)$$

In (4) numeric constants are chosen to satisfy following conditions: at pressure *p_m* = 0

$$k = k\_ref/3 \cdot (1 + \log 10) = 2/3 \cdot k\_ref,$$

at pressure *p_m* = *p_ref*

$$k = k\_ref/3 \cdot (1 + \log(90 + 10)) = k\_ref.$$

For hoses with relatively lower radial stiffness at lower pressures, another logarithmic dependence can be used:

$$k = k\_ref/2 \cdot (1 + \log(9 \cdot p\_m/p\_ref + 1)), \quad (7)$$

where

k = *k_ref*/2· (1 + log 1) = *k_ref* /2, if *p_m* = 0.

Hysteresis is described by

$$b \cdot \text{signv}(v, v\_lim), \quad (8)$$

where

hose wall radial deformation velocity

$$v = (x - xold)/\text{dt}, \quad (9)$$

signv = *v*/*v_lim*, when abs (*v*) < *v_lim*,

signv = 1, when *v* ≥ *v_lim*,

signv = −1, when *v* ≤ −*v_lim*.

Estimated value of *b* is chosen 2e–5 m based on (Sänger 1985, Figure 19). Value of *v_lim* is chosen 1e–4 m/s to ensure the function sign v to be continuous.

Equation for dynamics of hose wall (Ohashi and Hayashi 2014, Speicher *et al.* 2014) is presented as

$$h \cdot v + k \cdot x = p\_m \cdot A, \quad (10)$$

where damping force is expressed as *h*·*v*.

After substitution of *v* and *A* the equation is as

$$h \cdot (x - xold)/\text{dt} + k \cdot x = p\_m \cdot \pi \cdot (d + 2 \cdot x) \cdot l. \quad (11)$$

Now the mean radial deformation *x* of hose wall considering hysteresis is expressed as

$$x = (p\_m \cdot A_0 + h \cdot xold/\mathrm{dt})/(k + h/\mathrm{dt} - 2 \cdot \pi \cdot l \cdot p\_m) - b \cdot \mathrm{signv}(v, v\_lim), \tag{12}$$

where

$$A_0 = \pi \cdot d \cdot l. \tag{13}$$

3. Mathematical models of fluid physical properties

For used fluids HLP, density ρ_{15} at $T = 15$ °C, kinematic viscosity v_0 at different temperatures T in the interval from −60 to +60 °C and coefficients of fluid compressibility *Af*, *Bf* at $T = 20$ °C are taken from table. Physical properties of the fluid (kinematic viscosity *v*, density ρ, and compressibility factors of fluid *Af* and *Bf*) depending on the temperature *T* and the arithmetic mean pressure *p_m* are calculated. Formulae below considering fluid physical properties are based on (Murrenhoff 2005, Grossschmidt and Harf 2010).

Fluid kinematic viscosity *v* depending on relative content vol_0 of air in the fluid and mean pressure *pm* is expressed as

$$v = v_0 \cdot (1 + 1.5 \cdot vol_0) \cdot (1 + 3 \cdot 10^{-8} \cdot p\_m). \tag{14}$$

Density ρ of fluid depending on fluid type, temperature *T* °C, mean pressure *p_m* and relative content vol_0 of air is expressed as

$$\rho = (\rho_{15}/(1 + \alpha \cdot (T - 15))) \cdot (1 + (p\_m/(Af \cdot p\_m + Bf)) \cdot (1 - vol_0)), \tag{15}$$

where

$$\alpha = (4 + 0.1 \cdot T) \cdot 10^{-4}, \tag{16}$$

for fluids HLP10 and HLP15:

$$Af = 12.5 - 0.05 \cdot (T - 20), \tag{17}$$

$$Bf = (16.5 - 0.08 \cdot (T - 20)) \cdot 10^8, \tag{18}$$

for fluids HLP of higher kinematic viscosity:

$$Af = 14 - 0.05 \cdot (T - 20), \tag{19}$$

$$Bf = (18.4 - 0.10 \cdot (T - 20)) \cdot 10^8. \tag{20}$$

Volume of air *vol*, relative to the entire volume $V_F + V_A$, at mean pressure *p_m* is expressed as

$$vol = V_A/(V_F + V_A) = V_{A0} \cdot (p_0/(p\_m + p_0))^{1/ka} / (V_H \cdot (1 - p\_m/(Af \cdot p\_m + Bf))), \tag{21}$$

where volume of air in fluid at mean pressure *p_m*

$$V_A = V_{A0} \cdot (p_0/(p\_m + p_0))^{1/ka}, \tag{22}$$

volume of air in fluid at mean pressure $p\_m = 0$

$$V_{A0} = vol_0 \cdot \pi \cdot d^2 \cdot l/4, \tag{23}$$

hose volume

$$V_H = \pi \cdot (d + 2 \cdot x)^2 \cdot l/4, \tag{24}$$

hose volume at mean pressure $p\_m = 0$

$$V_{H0} = \pi \cdot d^2 \cdot l/4, \tag{25}$$

volume of air, relative to the entire volume $V_{F0} + V_{A0}$, at mean pressure $p\_m = 0$

$$vol_0 = V_{A0}/(V_{F0} + V_{A0}) = V_{A0}/V_{H0}, \tag{26}$$

fluid volume in hose at mean pressure *p_m*

$$V_F = (V_H - V_A) \cdot (1 - p\_m/(Af \cdot p\_m + Bf)), \tag{27}$$

fluid volume in hose at mean pressure $p\_m = 0$

$$V_{F0} = V_{H0} - V_{A0} = V_{H0} \cdot (1 - vol_0). \tag{28}$$

Volume elasticity of the fluid

$$C_F = \mathrm{d}V_F/\mathrm{d}p\_m = A \cdot \mathrm{d}x/\mathrm{d}p\_m \cdot (1 - p\_m/(Af \cdot p\_m + Bf)) - (V_H - V_A) \cdot Bf/(Af \cdot p\_m + Bf)^2 + V_{A0} \cdot (1 - p\_m/(Af \cdot p_m + Bf))/(ka \cdot (p\_m + p_0)) \cdot (p_0/(p\_m + p_0))^{1/ka}, \tag{29}$$

derivation of hose wall radial deformation *x* (12) from pressure *p_m*

$$\mathrm{d}x/\mathrm{d}p\_m = A_0/(k + h/\mathrm{dt} - 2 \cdot \pi \cdot l \cdot p\_m) + (p\_m \cdot A_0 + h \cdot xold/\mathrm{dt}) \cdot 2 \cdot \pi \cdot l/(k + h/\mathrm{dt} - 2 \cdot \pi \cdot l \cdot p\_m)^2. \tag{30}$$

Volume elasticity of the air in the fluid

$$C_A = -\mathrm{d}V_A/\mathrm{d}p\_m = V_{A0}/(ka \cdot (p\_m + p_0)) \cdot (p_0/(p\_m + p_0))^{1/ka}. \tag{31}$$

Sum of fluid and air volume elasticities

$$C = C_F + C_A. \tag{32}$$

4. Four-pole mathematical models with lumped parameters of the hose

Multi-pole mathematical models with lumped parameters of the hose as four-pole models of forms *H*, *G*, *Y* or *Z* (analogously to the electrical engineering) having various causalities (Grossschmidt 1971, Grossschmidt and Vanaveski 1971, Grossschmidt and Harf 2009) are shown in Figure 2. Models describing four causalities

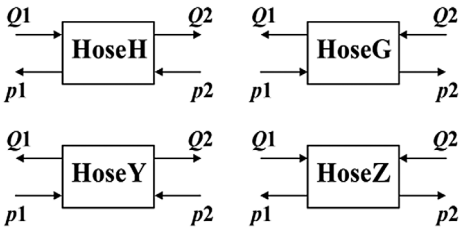

Figure 2. Four-pole models of forms *H*, *G*, *Y* and *Z* having various causalities.

enable to cover all the situations of using hoses when composing models of dynamic of complex fluid power systems.

All the models contain lumped resistance R (linear resistance RL and square resistance RT), inertial resistance of the flow L and volume elasticity C.

Formulas for calculating hydraulic flow resistances RL, RT and L (based on (Grossschmidt and Harf 2010) are as follows.

Hydraulic linear resistance

$$RL = \frac{2 \cdot Al \cdot l \cdot \nu \cdot \rho}{\pi \cdot (d + 2 \cdot x)^4} \tag{33}$$

Hydraulic square resistance

$$RT = \frac{8 \cdot \rho}{\pi^2 \cdot (d + 2 \cdot x)^4} \cdot \left(\varsigma + \lambda \cdot \frac{l}{(d + 2 \cdot x)} \right) \tag{34}$$

Hydraulic inertial resistance

$$L = 4 \cdot \rho \cdot \mathrm{l} / \left(\pi (\mathrm{d} + 2 \cdot x)^2 \right). \tag{35}$$

Formula for calculation of volume elasticity $\boldsymbol{C}$ is described in Chapter 3.

The fluid flow is characterised by the Reynolds number

$$Re = \nu \cdot d / \nu = 4 \cdot Q / (\pi \cdot d \cdot \nu). \tag{36}$$

Critical volumetric flow

$$Q_{\mathrm{Cr}} = \pi \cdot d \cdot \nu \cdot Re_{\mathrm{Cr}} / 4. \tag{37}$$

For example, if d = 0.016 m, ν = 46 e–6 m^2/s, and Re_{Cr} = 2300, then Q_{Cr} = 1.33e–3 m^3/s.

In general hydraulic tubes and hoses are chosen to ensure laminar flow. In practice fluid flow velocity is taken for pressure tubes and hoses in range 3…6 m/s.

The lumped resistance R takes into account linear and square dependence of the pressure drop on the volumetric flow. Square resistance RT takes into account hose bends, roughness of the inner surface, resistance of fittings, etc.

For the example above (parameters ζ = 2, λ = 0.04) pressure drops caused by proportional and square resistances RL and RT are shown in Figure 3.

The flow is laminar as volumetric flow values are lower than critical (1.33e–3 m^3/s). The proportion of pressure drop caused by square resistance is small.

As a result of analysis of various distributions of elements R, L, C in tube models the simplest structures of the four-pole models for tube dynamics, taking into account only the first natural frequency, are chosen as follows (Grossschmidt and Vanaveski 1971):

for form H in sequence C – R – L,
for form G in sequence L – R – C,
for form Y in sequence $L/2$ – $R/2$ – C – $R/2$ – $L/2$,
for form Z in sequence $C/2$ – $R/2$ – L – $R/2$ - $C/2$.

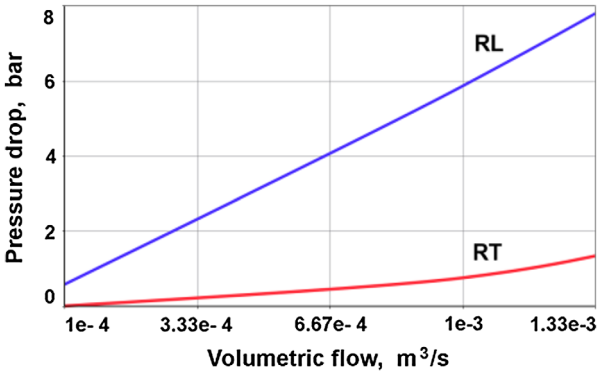

Figure 3. Pressure drops caused by *RL* and *RT*.

In order to achieve correspondence of natural frequency of the tube model with lumped parameters to the first natural frequency of the tube model with distributed parameters, the values of L and C have been corrected by coefficients

$$kL = kC = (2/\pi)^{(1/n)}. \tag{38}$$

For hoses the almost similar dependencies take place. If the hose model is considered consisting of n (n = 1, 3, 5, 7) models with lumped parameters, the correction coefficients are expressed as follows:

$$kL = kC = (2/\pi)^{(1/n)} + kn \cdot (n - 1), \tag{39}$$

where kn = 0.010…0.012.

Values of coefficient kn have been found as a result of calculation experiments with hose models consisting of n = 1…7 lumped models.

Correction coefficient kr is used to characterise difference of flow resistances under steady state conditions (kr = 1) and dynamics. Coefficient kr depends on fluid kinematic viscosity, inner diameter of hose, volumetric flow, type and amplitude of disturbance. Identification of all those dependencies is complicated. The correction coefficient kr for flow resistances RL and RT depending on n is obtained empirically as a result of calculation experiments and is expressed as

$$kr = kr1 - kr2 \cdot (n - 1), \tag{40}$$

where $kr1$ = 1.4, $kr2$ = 0.09…0.11.

5. Four-pole models of hydraulic hoses

5.1. Four-pole model of HoseH

Inputs: volumetric flow $Q1$, pressure $p2$.
Outputs: pressure $p1$, volumetric flow $Q2$.

For steady state conditions:

$$Q2 = Q1, \tag{41}$$

$$p1 = p2 + (RL + RT \cdot \mathrm{abs}(Q1)) \cdot Q1. \tag{42}$$

The four-pole model HoseH for dynamics composed from four-pole models of separate lumped components

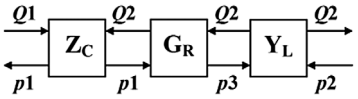

Figure 4. Four-pole structure of model HoseH for dynamics.

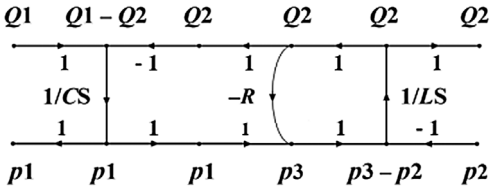

Figure 5. Oriented graph of the four-pole model HoseH for dynamics.

is represented in Figure 4. The corresponding oriented graph is shown in Figure 5.

For dynamics the mathematical expressions are as follows. To calculate Runge–Kutta coefficients for integration the differences $dQ2$ and $dp1$ of output variables are to be found.

Difference of output volumetric flow $Q2$

$$dQ2 = (dt/(kL \cdot\ L)) \cdot (p3 - p2), \tag{43}$$

where

$$p3 = p1 - R\ \cdot Q2, \tag{44}$$

$$R = kr \cdot (RL + RT \cdot \mathrm{abs}(Q2)). \tag{45}$$

Difference of output pressure $p1$

$$dp1 = (dt\ /(kC \cdot C)) \cdot (Q1 - Q2)\ . \tag{46}$$

The fourth-order classical Runge–Kutta method is used for calculating the values $Q2$ and $p1$:

$$Q2 = Q2old + \left(kq1 + 2 \cdot kq2 + 2 \cdot kq3 + kq4\right)/6, \tag{47}$$

$$p1 = p1old + (kp1 + 2 \cdot kp2 + 2 \cdot kp3 + \ kp4)/6. \tag{48}$$

Analogously, the four-pole model HoseG for dynamics composed from four-pole models of separate lumped components is represented in Figure 6.

5.2. Four-pole model of HoseY

Inputs: pressures $p1$, $p2$.
Outputs: volumetric flows $Q1$, $Q2$.

For steady state conditions:

$$Q1 = (-RL + (\mathrm{RL}^2 + 4 \cdot RT\ \cdot \mathrm{abs}(p1 - p2))^{1/2})/(2 \cdot RT), \tag{49}$$

$$Q2 = Q1. \tag{50}$$

The four-pole model HoseY for dynamics composed from four-pole models of separate lumped components

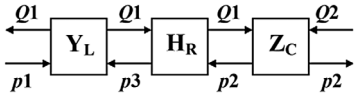

Figure 6. Four-pole structure of model HoseG for dynamics.

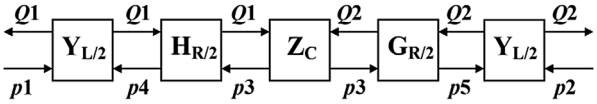

Figure 7. Four-pole structure of model HoseY for dynamics.

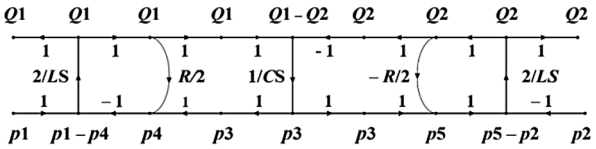

Figure 8. Oriented graph of the four-pole model HoseY for dynamics.

is represented in Figure 7. The corresponding oriented graph is shown in Figure 8.

For dynamics the mathematical expressions are as follows. To calculate Runge–Kutta coefficients for integration the differences $dQ1$, $dp3$ and $dQ2$ of output variables are to be found.

Difference of output volumetric flow $dQ1$

$$dQ1 = (dt\ /(kL \cdot L/2)) \cdot (p1 - p4)\ , \tag{51}$$

where

$$p4 = p3 + R1/2 \cdot Q1, \tag{52}$$

$$R1 = kr \cdot (RL + RT \cdot \mathrm{abs}\ (Q1))\ . \tag{53}$$

Difference of mean pressure $dp3$

$$dp3 = (dt/(kC \cdot \mathrm{C}\ )) \cdot (Q1 - Q2)\ . \tag{54}$$

Difference of output volumetric flow $dQ2$

$$dQ2 = (dt\ /(kL \cdot L/2)) \cdot (p5 - p2), \tag{55}$$

where

$$p5 = p3 - R2/2 \cdot\ Q2, \tag{56}$$

$$R2 = kr \cdot (RL + RT \cdot \mathrm{abs}\ (Q2))\ . \tag{57}$$

Equations for calculating values $Q1$, $p3$ and $Q2$ using Runge–Kutta method are:

$$Q1 = Q1old + (kq11 + 2 \cdot kq12 + 2 \cdot kq13 + kq14)/6, \tag{58}$$

$$p3 = p3old + (kp31 + 2 \cdot kp32 + 2 \cdot kp33 + kp34)/6, \tag{59}$$

$$Q2 = Q2old + (kq21 + 2 \cdot kq22 + 2 \cdot kq23 + kq24)/6. \tag{60}$$

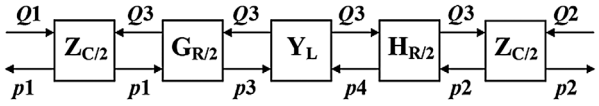

Figure 9. Four-pole structure of model HoseZ for dynamics.

Analogously, the four-pole model HoseZ for dynamics composed from four-pole models of separate lumped components is represented in Figure 9.

6. Programming environment

CoCoViLa (Grigorenko *et al.* 2005, Kotkas *et al.* 2011) is a programming environment, which supports declarative programming in a high-level language, automatic program synthesis and visual programming.

The CoCoViLa system supports a user in the definition of visual languages, including the specification of graphical objects, syntax and semantics of the language. CoCoViLa provides the user with a visual programming environment, which is automatically generated from the visual language definition.

Automatic synthesis of programs is a technique for the automatic construction of programs from the knowledge available in specifications.

When a visual scheme is composed by the user, the following steps – parsing, planning and code generation – are fully automatic. The compiled program then provides a solution for the problem specified in the scheme.

7. Simulation process organisation

Simulation of dynamics of hydraulic hoses includes:

- calculation of transient responses;
- calculation of frequency characteristics based on transient responses of sinusoidal input.

For each particular simulation, a task description must be composed using visual tools provided by CoCoViLa. Simulation task contains visual multi-pole models of hydraulic hoses, inputs, graphical outputs, clock, simulation manager, etc.

It is easy to solve various computing problems on each simulation task due to automatic program synthesis.

To follow the system behaviour in time, the concept of state is introduced as a couple of variables, characterising the system at certain moment of time (at certain time step).

Dynamic calculations proceed from the initial state to the final state. The key procedure here is the procedure of computing the next state values from the (known) current state (or several previous states) values.

Calculation of transient responses is organised by simulation manager *dynamic_Process*. When calculating frequency characteristics, simulation manager *dynamic_Process* is used as a multi-level organiser.

Using multi-pole models allows using inner and outer variables of components in different roles. All the variables described in a multi-pole model of the component are inner variables. Poles of a multi-pole model are both, inner and outer variables of the component.

Using multi-pole models allows to perform calculations at two separate levels:

- at the lower level are those which take place in each component model between inner variables of the component;
- at the higher level are those which take place in the model of the entire fluid power system and include only outer variables (poles) of components.

Model of the fluid power system is built up from multi-pole models of components by connecting necessary poles.

When analysing the fluid power system models one can see that loop dependences can appear between outer variables of components. The special iteration procedure is used for solving these loop dependencies. Usually we split one variable in each loop, provide it with approximate initial value and try to refine it by re-computing. The re-computing algorithm for each split variable is automatically synthesised by the CoCoViLa system.

In more detail the computing process organisation is considered in (Grossschmidt and Harf 2016).

8. Simulation of transient responses of hydraulic hoses

In this chapter, simulation of transient responses of hydraulic hoses caused by a step disturbance is considered.

Four-pole mathematical models with lumped parameters of forms *H*, *G*, *Y* or *Z* described in Chapter 4 are used.

In the example below, simulation task (Figure 10) and resulting graphs (Figure 11) of transient responses of a hose consisting of $n = 7$ sequentially connected four-pole models of form H are considered.

Simulations are performed under following conditions.

Hose models: HoseH_Q – model of form H. All the output volumetric flows Q2e of models HoseH_Q are calculated using iterations for solving loop dependencies (see Chapter 7).

Inputs: constant volumetric flow Q1 = 5e–4 m^3/s, step input pressure *p*2: mean = 1e7 Pa, step = 1e6 Pa.

Simulation parameters: time step *d*t = 1e–6 s, calculation steps 1e5.

In all the following examples (except in Chapter 9.2) the hose with following parameters is used: $l = 2/n$ m, $d = 0.016$ m, $p\_ref = 1e7$ Pa, $x\_ref = 0.0004$ m, $b = 2e{-}5$ m, $h = 200$ Ns/m, $kn = 0.011$, $kr1 = 1.4$, $kr2 = 0.10$.

Physical properties of working fluid (density ρ, kinematic viscosity ν and coefficients of fluid

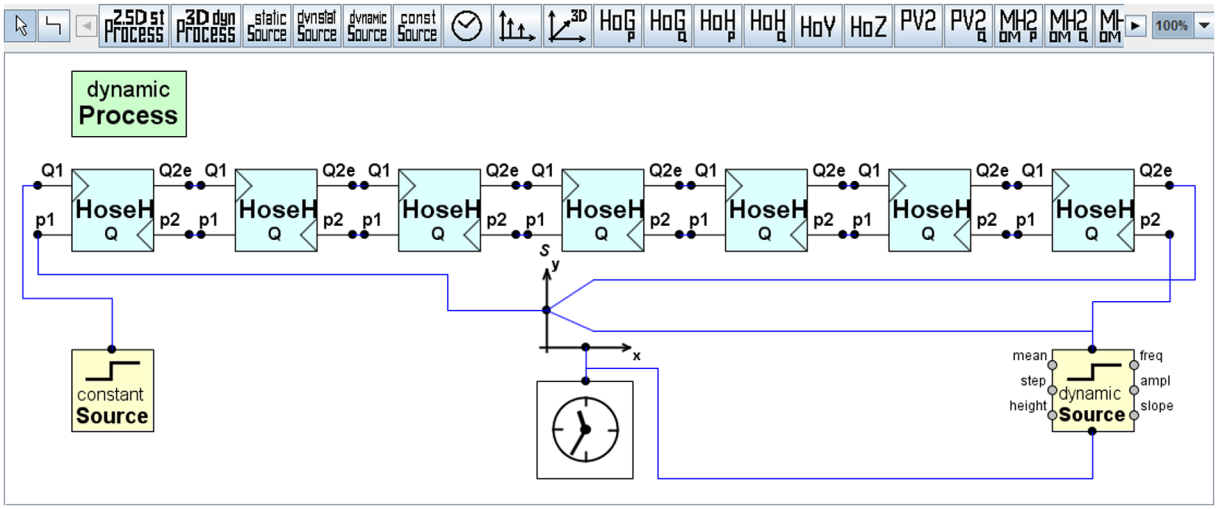

Figure 10. Simulation task of the hydraulic hose, represented by $n = 7$ models of form H.

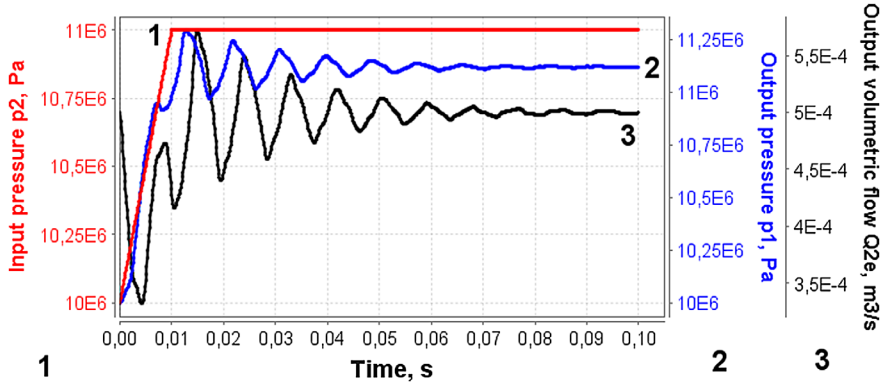

Figure 11. Graphs of transient responses of HoseH ($n = 7$).

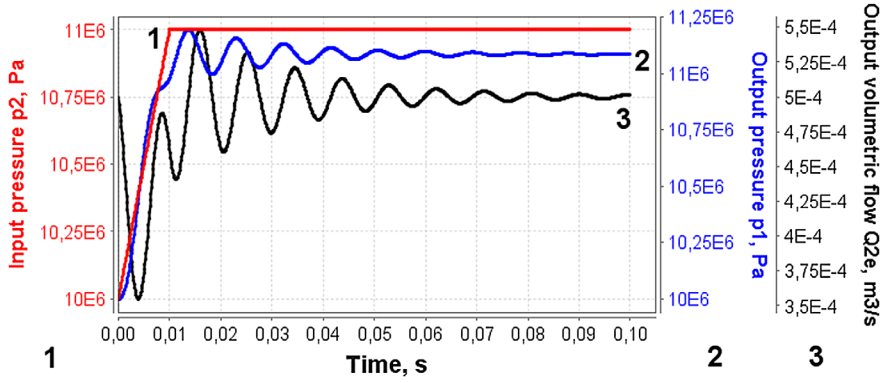

Figure 12. Graphs of transient responses of HoseH ($n = 1$).

compressibility *Af and Bf*) are calculated at each simulation step depending on average of input and output pressure in the component and fluid temperature. In all the simulations hydraulic fluid HLP46 at temperature 40 °C is used. Kinematic viscosity at temperature 40 °C ν = 46e–6 m^2/s, density at temperature 15 °C ρ_{15} = 875 kg/m^3, volume of air, relative to the entire volume at $p\_m = 0$, $vol_0 = 0.08$.

Step change 1e6 Pa of input pressure $p2$ = 10e6 Pa (graph 1) causes damped oscillations (frequency ~106 Hz) of output pressure $p1$ (graph 2) and output volumetric flow $Q2$ (graph 3) with different phase shift. The shape of oscillations is influenced by higher natural frequencies.

When simulating larger fluid power systems it is reasonable to use hose model as simple as possible. In the following example, the model consisting of one hose model of form H (taking into account only the first natural frequency of the hose) is used. The simulation results are shown in Figure 12.

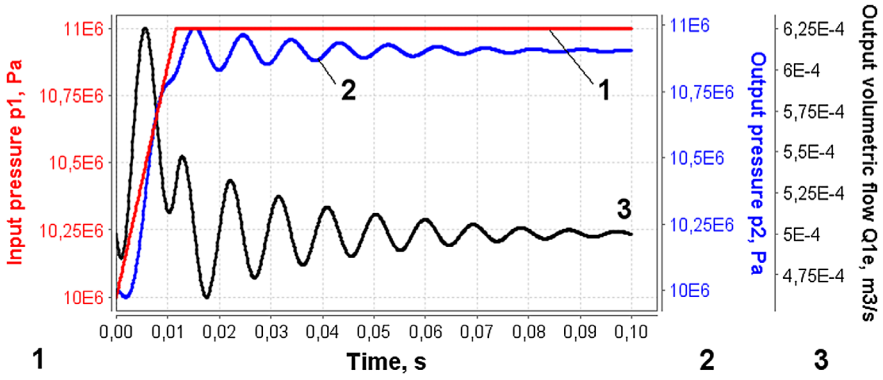

Figure 13. Graphs of transient responses of HoseG ($n = 1$).

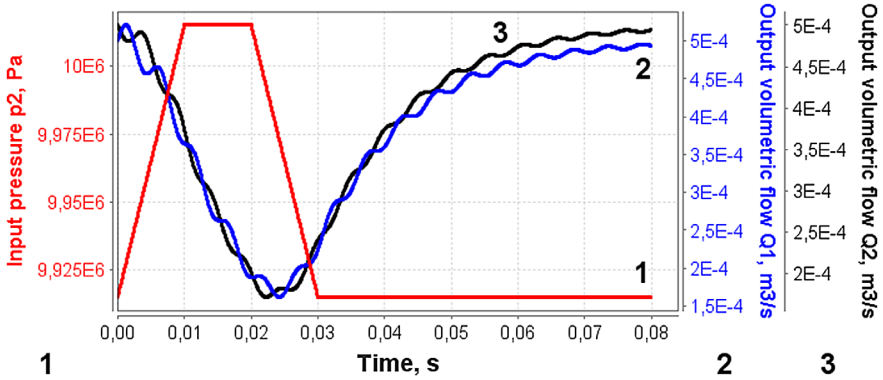

Figure 14. Graphs of transient responses of HoseY ($n = 1$).

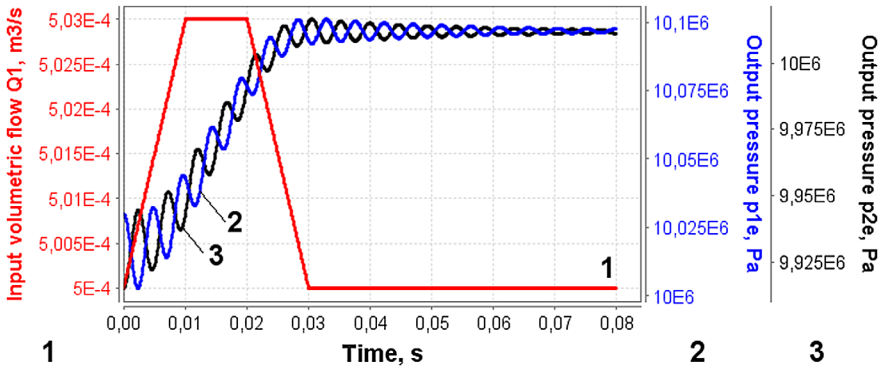

Figure 15. Graphs of transient responses of HoseZ ($n = 1$).

The oscillations in Figure 12 are of the same natural frequency (~106 Hz), amplitudes and damping time as the oscillations in the example for $n = 7$. It is due to coefficient *kn* for correction of natural frequency and coefficient *kr* for correction of flow resistances (influencing process duration) (see Chapter 4).

Based on the results for hoses with parameters from the example above it is reasonable to use one four-pole model with lumped parameters representing a hose model.

In Figures 13–15 results of simulation of dynamic responses caused by step change of input pressure for models of forms HoseG, HoseY and HoseZ are shown.

In Figure 13, step change 1e6 Pa of input pressure $p1$ = 10e6 Pa (graph 1) causes damped oscillations with frequency ~106 Hz of output pressure $p2$ (graph 2) and output volumetric flow $Q1$ (graph 3) with different phase shift.

In Figure 14, impulse disturbance of input pressure $p2$ (mean 9.915e6 Pa, height of the impulse 1e5 Pa, duration of the impulse, disturbance rise and drop durations 0.01 s) (graph 1) causes output volumetric flows $Q1$ and $Q2$ (graph 2 and 3) to drop down with some delay and return to initial level with damped oscillations (frequency ~195 Hz).

In Figure 15, impulse disturbance of input volumetric flow $Q1$ (mean 5e–4 m^3/s, height of the impulse

3e–6 m³/s, duration of the impulse, disturbance rise and drop durations 0.01 s) (graph 1) causes output pressures *p*1e and *p*2e (graph 2 and 3) in opposite phases to increase and take a new higher level with damped oscillations (frequency ~210 Hz).

For the hose models of forms *G* and *H*, if quarter length of the wave fits with the length of the hose the resonance takes place. For models of forms *Y* and *Z*, if half length of the wave fits with the length of the hose the resonance takes place. For the models without damping (flow resistances are not considered) the first resonance frequency of models of forms *Y* and *Z* is twice higher than the first resonance frequency of models of forms *G* and *H*.

9. Simulation of frequency responses of hydraulic hoses

9.1. Simulation task

In Figure 16 two-level simulation task for calculating logarithmic amplitude-frequency responses of hose (model HoseH_Q) is shown.

At the lower level, transient responses of outputs (*p*1 and *Q*2e of model HoseH_Q) in case of input sinusoidal pressure *p*2 of given frequency *freq* and amplitude *Ap*2 (*ampl* in Figure 16) are calculated.

At the higher level, maximums of amplitudes *max_Ap*1 and *max_AQ*2e (*maxl* in Figure 16) of all calculated *p*1 and *Q*2e are found. Transient responses caused by sinusoidal input require some time to stabilise. To get reliable results the initial phases of transient responses are not considered when finding *maxAp*1 and *max_AQ*2e. Logarithmic amplitude ratios 20log(*max_Ap*1/*Ap*2) and 20log(*max_AQ*2e/*Ap*2) in dB are calculated for input disturbances in all the diapason of frequencies.

Two-level simulation process for organising calculations of amplitude-frequency responses is described in the model *dynamic_Process*. Calculations of logarithmic amplitude ratios are described in the model *Maxlog*.

Simulations are performed under following conditions.

Model: HoseH_Q – hose type H.

Hose parameters: see Chapter 8.

Inputs: constant volumetric flow *Q*1 = 5e–4 m³/s, sinusoidal pressure *p*2: mean 1e7 Pa, amplitude *Ap*2 = 3e5 Pa, frequency 2…150 Hz.

Simulation parameters: calculation steps 2e5 for each particular transient response, calculation steps 300 for frequencies, simulation time step 1e–6 s.

Results of calculations of logarithmic amplitude-frequency responses 20log(*max_AQ*2e/*Ap*2) (graph 1) and 20log(*max_Ap*1/*Ap*2) (graph 2) are presented in Figure 17.

Simulated resonance frequency is 106.0 Hz for pressure *p*1 and 106.7 Hz for volumetric flow *Q*2e. Logarithmic amplitude ratios at resonance are: 20log(*max_AQ*2e/*Ap*2)=– 168.75 dB and 20log(*max_Ap*1/*Ap*2) = 17.43 dB.

In Figure 18, calculated graphs of logarithmic amplitude-frequency responses of a hose of length 2 m consisting of *n* = 7 sequentially connected four-pole models of form H are presented.

Here seven resonances and seven anti-resonances take place. Calculation of these graphs is very time consuming, it takes 799 s (120 s when calculating graphs in Figure 17) on high performance laptop.

Amplitude ratios of higher resonance frequencies are dropping down.

Results of calculations of logarithmic amplitude-frequency responses 20log(*max_AQ*1/*Ap*2) (graph 1) and

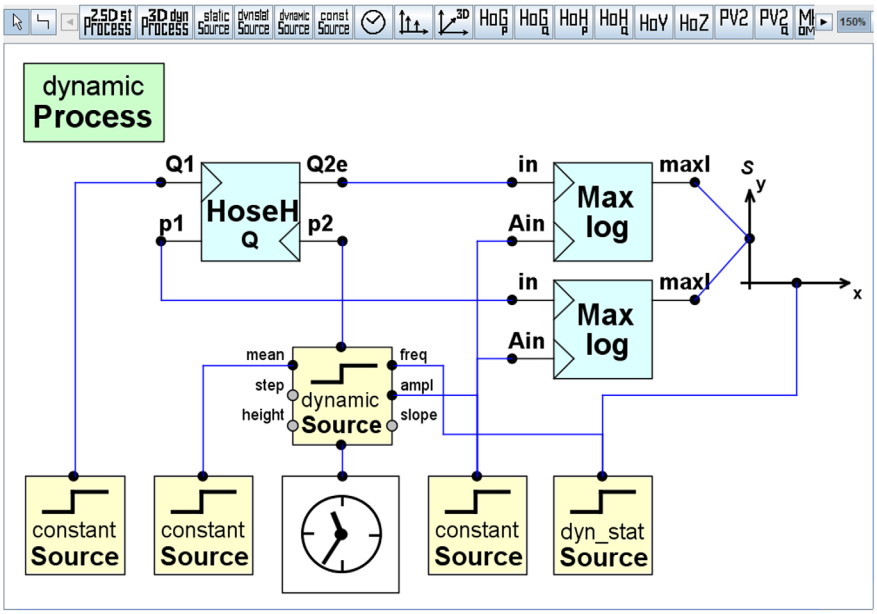

Figure 16. Simulation task for calculating logarithmic amplitude-frequency responses of hose (*n* = 1).

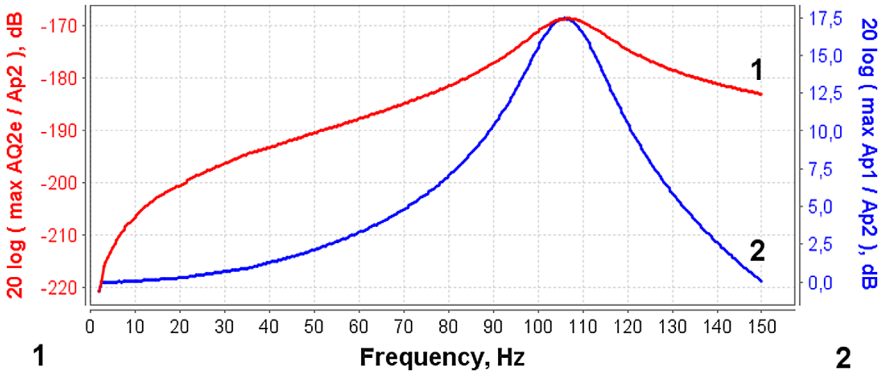

Figure 17. Simulated logarithmic amplitude-frequency responses of HoseH ($n = 1$).

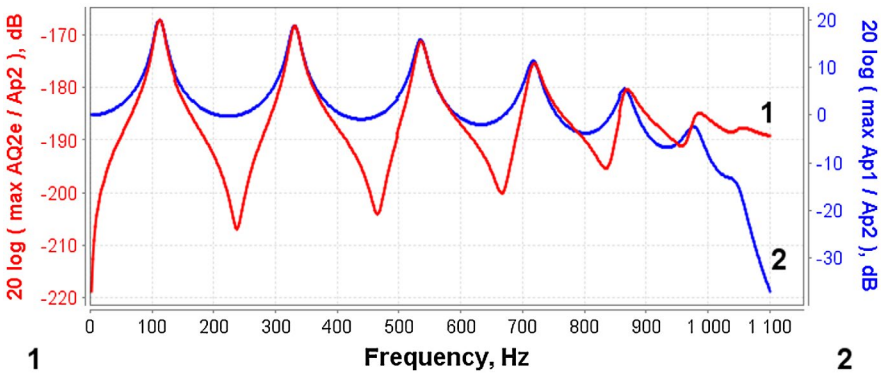

Figure 18. Simulated logarithmic amplitude-frequency responses of HoseH ($n = 7$).

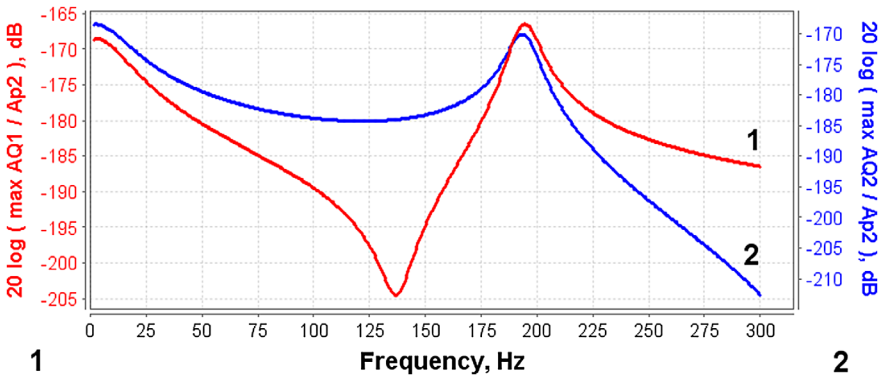

Figure 19. Simulated logarithmic amplitude-frequency responses of HoseY ($n = 1$).

20log($max\_AQ2/Ap2$) (graph 2) using model HoseY are presented in Figure 19.

Simulated resonance frequency for $Q1$ is 192.6 Hz and for $Q2$ is 195.0 Hz. Logarithmic amplitude ratios at resonance are: 20log ($max\_AQ1/Ap2$) = −166.0 dB and 20log ($max\_AQ2/Ap2$) = −169.7 dB.

Based on the results of simulations concerning examples above one can say that using in simulations of complex fluid power systems one multi-pole model for representing hoses of given parameters is reasonable if frequencies in the system do not exceed ~150 Hz when using models of forms H or G and ~300 Hz when using models of forms Y or Z.

9.2. Comparison with experiments

The results of measured frequency responses of a hose are taken from (Sänger 1985). The experimental device contains hydraulic pump, pressure relief valve, accumulator and impulse generator. All the components of the experimental device influence to the dynamic behaviour of the hose. Steel wire reinforced high pressure hose DN 10 (inner diameter 0.01 m) of length 1 m was used in tests. The end of the hose was closed (input volumetric flow $Q1 = 0$). Dependencies of resonance frequency (Sänger 1985, Figure 50) and logarithmic amplitude ratio at resonance (Sänger 1985, Figure 49) on input mean pressure

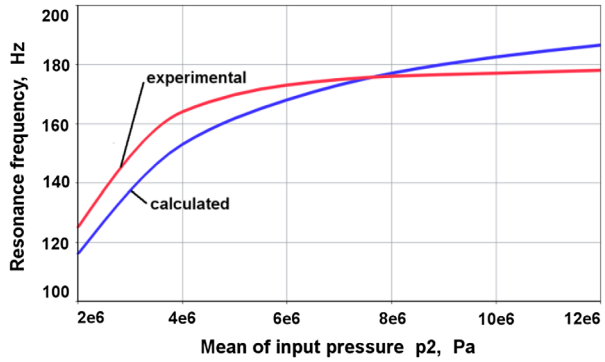

Figure 20. Experimental and calculated resonance frequencies depending on input pressure *p*2.

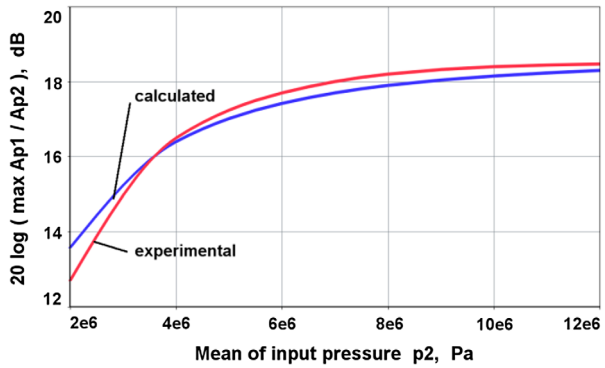

Figure 21. Experimental and calculated logarithmic amplitude ratios at resonance depending on input pressure *p*2.

were presented. The type, kinematic viscosity and temperature of fluid, relative volume of air in fluid, stiffness of hose wall, damping coefficient of hose wall deformation and amplitude of disturbances were not specified.

To compare measured results of experiments and calculated results a simulation task similar to Figure 16 (model HoseH_Q) was composed where input volumetric flow $Q1 = 0$ and pressure $p2$ of sinusoidal form for different mean values was used as input.

Hose parameters were taken from experiment: length $l = 1$ m and inner diameter $d = 0.01$ m. Parameters used in simulations are: fluid HLP46, $T = 40$ °C, $vol_0 = 0.10$, $x\_ref = 0.00034$ m, $kr = 0.8$, amplitude of disturbances $Ap2 = 5e5$ Pa.

Experimental and simulated dependencies are shown in Figures 20 and 21.

Both calculated resonance frequencies and logarithmic amplitude ratios at resonance slightly differ from experimental results. The differences might be caused by lack of information about the experimental device and values of fluid and hose parameters.

9.3. Simulation of resonance frequencies

The simulations below are performed using the simulation task and parameters described in Section 9.1. Resonance frequencies are obtained from the resulting

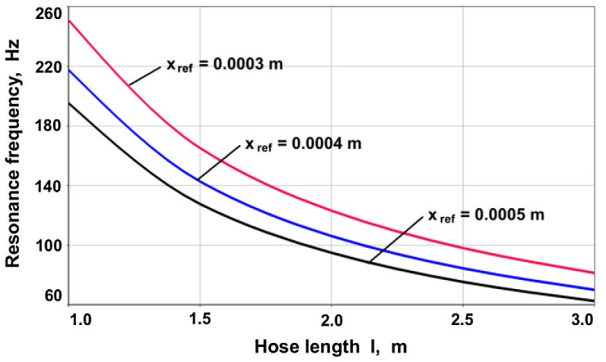

Figure 22. Resonance frequency depending on hose length *l*.

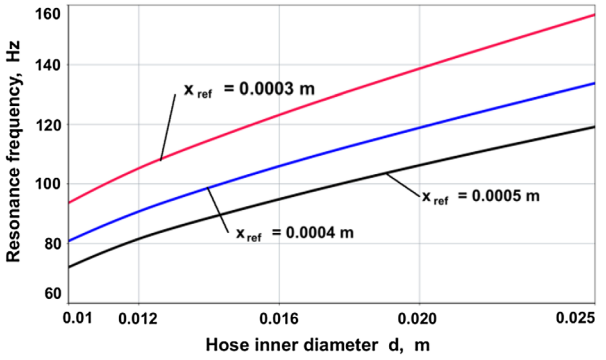

Figure 23. Resonance frequency depending on hose inner diameter *d*.

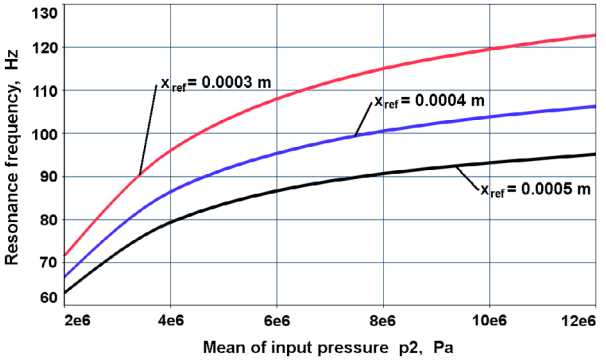

Figure 24. Resonance frequency depending on mean of input pressure *p*2.

graphs of simulations. Resonance frequencies are found for various hose lengths *l* (Figure 22), hose inner diameters *d* (Figure 23) and means of input pressures *p*2 (Figure 24).

Resonance frequency is lower on bigger hose length *l*. On higher hose wall stiffness (lower reference radial deformation of hose wall *x_ref*) the resonance frequency is higher.

Resonance frequency is higher at bigger hose inner diameters *d*. On bigger hose wall stiffnesses the resonance frequency is higher.

In Figure 24, the influence of *p*2 to resonance frequency is more evident at lower pressures ($p2 < 4e6$ Pa).

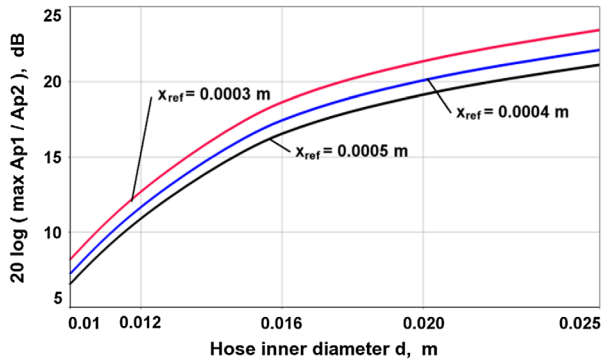

Figure 25. Logarithmic amplitude ratios at resonance depending on hose inner diameter *d*.

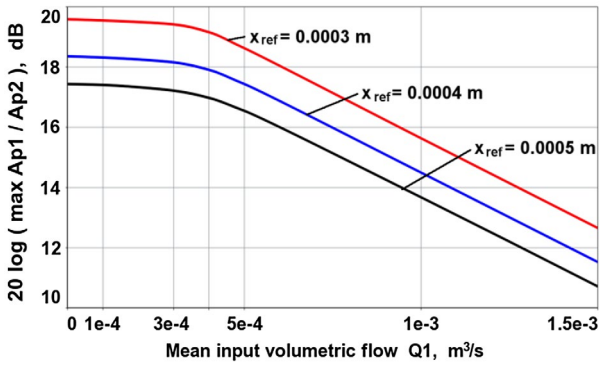

Figure 27. Logarithmic amplitude ratios at resonance depending on mean of input volumetric flow *Q*1.

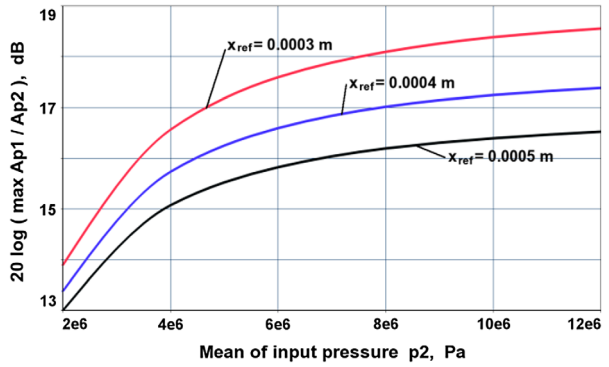

Figure 26. Logarithmic amplitude ratios at resonance depending on mean of input pressure *p*2.

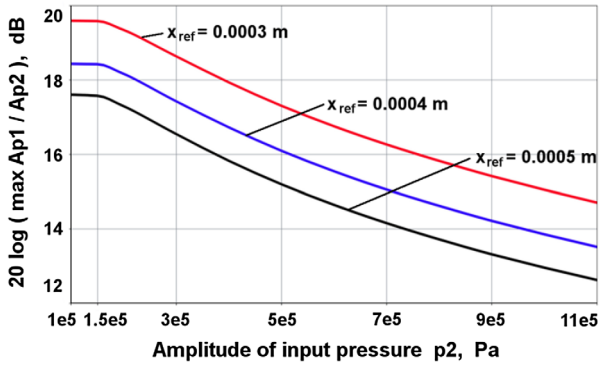

Figure 28. Logarithmic amplitude ratios at resonance depending on amplitude of input pressure *p*2.

Resonance frequency drops as volume elasticity of air in working fluid is growing and stiffness of the hose wall is dropping.

As a result of performed simulations influence of kinematic viscosity of fluid v, fluid temperature T, relative volume of air vol_0, damping coefficient of hose wall h, correction coefficient kr, input volumetric flow $Q1$ and amplitude of input pressure $Ap2$ to resonance frequency turned out to be not remarkable and are not presented.

9.4. Simulation of logarithmic amplitude ratios at resonance

The simulations below are performed using the simulation task and parameters described in Section 9.1. Logarithmic amplitude ratios at resonance are obtained from the resulting graphs of simulations.

In Figures 25 and 26 logarithmic amplitude ratios 20log (*max_Ap*1/*Ap*2) at resonance are higher at bigger hose inner diameters d and at higher values of mean input pressure $p2$. At smaller reference radial deformation of hose wall *x_ref* the logarihtmic amplitude ratios are higher. In Figure 26, lower values of amplitude ratios at lower mean input pressures are caused by greater volume elasticity of air in working fluid and lower stiffness of the hose wall.

In Figure 27, at smaller input volumetric flows ($Q1$ < 3e–4 m^3/s) logarithmic amplitude ratios at resonance are almost constant, thereafter the ratios drop linearly.

In Figure 28, at smaller amplitudes of input pressure ($Ap2$ < 1.5e5 Pa) logarithmic amplitude ratios at resonance are constant, thereafter the ratios drop.

A number of simulations were performed which results are not presented. Logarithmic amplitude ratios 20log(*max_Ap*1/*Ap*2) at resonance are almost linearly depending (decreasing from ~21 to ~15 dB) on correction coefficient kr = 0.8…1.8, hose length l = 1…3 m and kinematic viscosity of fluid v = 10…100 mm^2/s. They are higher at smaller reference radial deformation of hose wall *x_ref*. Influence of relative volume of air vol_0 and damping coefficient of hose wall h to amplitude ratios turned out to be not remarkable.

10. Conclusions

Multi-pole models with lumped parameters for hydraulic hoses, having various causalities, have been proposed. Four-pole models for dynamics consisting of separate elementary components were described. Corresponding oriented graphs were composed and calculation formulas were presented. Non-linear mathematical model of radial deformation of hose wall was presented.

CoCoViLa programming environment, which supports visual programming and automatic program synthesis is used as a tool for describing mathematical multi-pole models and performing simulations.

Calculations of transient responses of hoses described by four-pole models with various causalities were considered.

Multi-level simulation process has been proposed for calculating resonance frequencies and logarithmic amplitude ratios at resonance. Automatic calculations of transient responses in case of sinusoidal disturbances in the whole range of input frequencies are used in the simulations.

Frequency characteristics were presented for dependencies on various parameters such as hose length, hose inner diameter, mean pressure, mean volumetric flow, amplitude of input pressure, kinematic viscosity of fluid, reference radial deformation of hose wall, content of air in fluid and fluid temperature.

Comparison with experimental results (taken from literature) was presented.

Using hose four-pole models with lumped parameters for dynamics was analysed and justified in the paper. Using such models enables to simplify model-based simulation in development of various fluid power systems.

Nomenclature

A_0	hose inner area at mean relative pressure $p\_m = 0$
A	hose inner area depending from mean relative pressure p_m
Af	coefficient of fluid compressibility, depending on fluid and temperature
Bf	coefficient of fluid compressibility, depending on fluid and temperature, 1/Pa
Al	hydraulic friction coefficient of laminar flow (in ideal case Al = 64, in practice Al = 75)
$Ap2$	amplitude of input pressure $p2$
A_ref	reference hose inner area
B	half of hysteresis of hose wall deformation
C	volume elasticity of fluid with air in hose
C_A	volume elasticity of air in hose
C_F	volume elasticity of fluid in hose
d	inner diameter of the hose at $p_m = 0$
dt	simulation time step
f	frequency
h	viscous damping coefficient of hose wall
k	radial stiffness of hose wall
k_ref	reference radial stiffness of hose wall
ka	polytrope exponent
kC	correction coefficient for fluid volume elasticity in dynamic at n = 1
kL	correction coefficient for fluid inertial resistance in dynamic at n = 1
kn	correction coefficient for fluid volume elasticity and inertial resistance in dynamic if n > 1
kp, kq	Runge–Kutta coefficients
kr	correction coefficient for flow resistances in dynamic
$kr1, kr2$	coefficients in expression of kr
l	hose length
L	inertia resistance of flow
max_Ap1	maximum amplitude of pressure $p1$
n	number of joint similar four-pole models in sequence
$p1, p2$	relative pressures at left and right port of hose at current time step
$p3, p4, p5$	intermediate relative pressures
$p1old, p2old$	relative pressures at left and right port of hose at previous time step
p_0	atmospheric (absolute) pressure
p_m	mean relative pressure
p_ref	reference relative pressure
Re	Reynolds number
Re_{Cr}	critical Reynolds number
RL, RT	hydraulic linear and square flow resistance
$Q1, Q2$	volumetric flows at current time step at left and right port of hose
$Q3$	intermediate volumetric flow
$Q1old, Q2old$	volumetric flows at left and right port of hose at previous time step
Q_{cr}	critical volumetric flow
S	differentiation operator
T	fluid temperature, °C
V_{A0}	volume of air in fluid at $p\_m = 0$
V_A	volume of air in fluid depending on pressure p_m
V_{F0}	fluid volume in hose at $p\_m = 0$
V_F	fluid volume in hose depending on pressure p_m
V_{H0}	hose inner volume at $p\_m = 0$
V_H	hose inner volume depending on pressure p_m
v	fluid flow velocity
v	hose wall deformation velocity
v_lim	hose wall deformation velocity limit for function signv
vol	volume of air, relative to the entire volume, depending on pressure p_m
vol_0	volume of air, relative to the entire volume, at $p\_m = 0$
x	inner mean radial deformation of hose at current time step
x_0	initial mean radial deformation of hose wall
$xold$	inner mean radial deformation of hose wall at previous time step
x_ref	reference inner mean radial deformation of hose wall

α	isobaric thermal expansion coefficient
ζ	local resistance coefficient
λ	hydraulic friction coefficient at turbulent flow
ν_0	fluid kinematic viscosity at $p\_m = 0$
ν	fluid kinematic viscosity at pressure p_m and relative volume of air vol_0
ρ_{15}	fluid density at temperature 15 °C, pressure $p\_m = 0$ and relative volume of air $vol_0 = 0$
ρ	fluid density at temperature T, pressure p_m and relative volume of air vol_0

Disclosure statement

No potential conflict of interests was reported by the authors.

Funding

This research was supported by the Estonian Ministry of Research and Education institutional research grant number grant no. IUT33–13, the Innovative Manufacturing Engineering Systems Competence Centre IMECC and Enterprise Estonia (EAS) and European Union Regional Development Fund (project EU48685).

Notes on contributors

Gunnar Grossschmidt Dipl. Eng. degree obtained from Tallinn University of Technology in 1953. Candidate of Technical Science degree (PhD) received from the Kiev Polytechnic Institute in 1959. His research interests are concentrated around modelling and simulation of fluid power systems. His list of scientific publications contains 94 items. He has been lecturing at the Tallinn University of Technology 55 years, as Assistant, Lecturer, Associate Professor, Head of the chair of Machine Design and Senior Researcher.

Mait Harf Dipl. Eng. degree obtained from Tallinn University of Technology in 1974. Candidate of Technical Science degree (PhD) received from the Institute of Cybernetics, Tallinn in 1984. His research interests are concentrated around intelligent software design. He worked on methods for automatic (structural) synthesis of programs and their applications to knowledge based programming systems such as PRIZ, C-Priz, ExpertPriz, NUT and CoCoViLa.

References

Chipperfield, K. and Vance, J., 2002. Stiffness testing of hydraulic hoses. *In*: *Proceedings of ASME 28th design automation conference*, Montréal, Canada, 2, 283–287.

Grigorenko, P., Saabas, A. and Tyugu, E., 2005. COCOVILA – compiler – compiler for visual languages. *In*: *Proceedings of the 5th workshop on language descriptions, tools and applications*, (Edinburgh), vol. 141, n. 4 of Electron. Notes in Theor. Comput. Sci., 137–142, Elsevier.

Grossschmidt, G.T., 1971. Calculating frequency responses of tubes with distributed parameters of hydraulic drives of machine tools. *Proceedings of Tallinn Polytechnical Institute nr.*, 317, 147–156 (in Russian).

Grossschmidt, G.T. and Vanaveski, J.J., 1971. Calculating Frequency Responses of Tubes with Lumped Parameters of Hydraulic Drives of Machine Tools. *Proceedings of Tallinn Polytechnical Institute nr.*, 317, 157–165 (in Russian).

Grossschmidt, G. and Harf, M., 2009. COCO-SIM – object-oriented multi-pole modelling and simulation environment for fluid power systems, part 1: fundamentals. *International journal of fluid power*, 10 (2), 91–100.

Grossschmidt, G. and Harf, M., 2010. Simulation of hydraulic circuits in an intelligent programming environment (Part 1, Part 2). *In*: *Proceedings of the 7th international conference of DAAAM Baltic "Industrial Engineering"*, April 22–24, Tallinn, Estonia, 148–161.

Grossschmidt, G. and Harf, M., 2016. Multi-pole modelling and simulation of an electro-hydraulic servo-system in an intelligent programming environment. *International journal of fluid power*, 17 (1), 1–13.

Johnston, D.N., 2006. A time-domain model of axial wave propagation in liquid-filled flexible hoses. *Proceedings of the institution of mechanical engineers, Part I: Journal of systems and control engineering*, 220 (7), 517–530.

Johnston, D.N., Way, T.M. and Cone, K.M., 2010. Measured dynamic properties of flexible hoses. *Journal of vibration and acoustics*, 132 (2), 021011, 8 p.

Kajaste, J., 1998. Experiences in simulating pipeline dynamics in large-scale mechatronic fluid power systems. *In*: *Proceedings of the 2nd Tampere international conference on machine automation ICMA'98*, September 15–18, Tampere University of Technology, Finland, 789–803.

Kannisto, S. and Virvalo, T., 2002. Hydraulic pressure in long hose. *In*: *Bath Workshop on power transmission and motion control (PTMC 2002)*. Professional Engineering Publications, Bath, UK, 165–176.

Kojima, E., Yamazaki, T. and Shinada, M., 2006. Development of a new simulation technique based on the modal approximation for fluid transients in complex pipeline systems with time-variant nonlinear boundary conditions. *Journal of fluids engineering*, 129 (6), 791–798, November 24.

Korobochkin, B. and Komitowski, M., 1968. Transfer functions of fluid power system pipelines in distributed and lumped parameters. *Machine science*, 4, 37–44 (in Russian).

Kotkas, V., *et al.*, 2011. CoCoViLa as a multifunctional simulation platvorm. *SIMUTOOLS 2011–4th International ICST conference on simulation tools and techniques*, March 21–25, Barcelona, Spain, ICST, 1–8.

Krus, P., Weddfelt, K. and Palmberg, J.-O., 1994. Fast pipeline models for simulation of hydraulic systems. *Journal of dynamic systems, measurement, and control*, 116 (1), 132–136(Mar 01)..

Mäkinen, J., Piché, R. and Ellman, A., 2000. Fluid Transmission line modeling using a variational method. *Journal of dynamic systems, measurement, and control*, 122 (1), 153–162, 03.2000.

Manning, N., 2005. *Hydraulic control systems*. Hoboken, NY: Wiley.

Murrenhoff, H., 2005. Fundamentals of fluid technology, Vol. 1: Hydraulics, 4. neu überarbeitete Auflage. Institut für fluidtechnische Antriebe und Steuerungen, Aachen (in German).

Muto, T., Yamada, H. and Kato, H., 1996. A fast and convenient method for simulating transient response of fluid lines with viscoelastic pipe walls. *In*: 12. *Aachener*

Fluidtechnisches Kolloquium 12–13. März, Band 2, 257–268.

Ohashi, S. and Hayashi, M., 2014. The simple measurement of the viscoelastic characteristic in a viscoelastic pipe. *In*: *Proceedings of the 9th international fluid power conference*, 9. IFK, March 24–26, Aachen, Germany, Vol. 1, 498–509.

Pršić, D., Nedić, N. and Dubonjić, L., 2011. Modeling and simulation of hydraulic long transmission line by bond graph. *Proceedings of the VII triennial international conference heavy machinery – HM*, 7 (3), 41–46.

Sänger, J., 1985. Hydraulic hose lines – calculation of braids and simulation of transmission behavior. Der Fakultät für Maschinenwesen der Rheinisch-Westfälischen Hochschule Aachen genehmigte Dissertation zur Erlangung des akademischen Grades eines Doktor-Ingenieurs, 139 S (in German).

Soumelidis, M., *et al.*, 2005. A comparative study of modelling techniques for laminar flow transients in hydraulic pipelines. *In: JFPS*, 2005-01-01.

Speicher, T., Baum, H. and Gessat, J., 2014. New system optimization opportunities by simulation based line tuning. *In*: *Proceedings of the 9th international fluid power conference*, 9. IFK, March 24-26, Aachen, Germany, Vol. 1, 542–553.

Stecki, J.S. and Davis, D.C., 1986. Fluid transmission lines – distributed parameters models. Part 1: a review of the state of the art. *Proceedings of the institution of mechanical engineers, part a: power and process engineering*, 200 (4), 215–228.

Taylor, S.E.M., Johnston, D.N. and Longmore, D.K., 1997. Modelling of transient flow in hydraulic pipelines. *Proceedings of the institution of mechanical engineers, Part I: Journal of systems and control engineering*, 211 (6), 447–456.

Watton, J., 2014. *Fundamentals of fluid power control*. Cambridge: Cambridge University Press.

Xu, Y., Johnston, D.N., Jiao, Z. and Plummer, A.R., 2014. Frequency modelling and solution of fluid-structure interaction in complex pipelines. *Journal of sound and vibration*, 333 (10), 2800–2822.